UDC 621.313.332 https://doi.org/10.36296/1819-8058.2025.3(82).184-192

DEVELOPMENT AND APPLICATION OF THE ADJUSTABLE LOAD SHARING COEFFICIENTS METHOD FOR LOAD SHARING CONTROL BETWEEN PARALLEL OPERATING GENERATORS IN ISOLATED POWER GENERATION SYSTEMS

Received Sept. 01, 2025; accepted Sept. 22, 2025
Available online Sept. 30, 2025

Mazurenko L.[1], Dzhura O.[2], Shykhnenko M.[3]

Author for correspondence: Mazurenko Leonid,
e-mail: 3662491@gmail.com

[1] Dr. of Tech. Sciences, prof.
https://orcid.org/0000-0002-7059-249X

[2] Cand. of Tech.Science
https://orcid.org/ 0000-0002-0224-3351

[3] Cand. of Tech.Science
https://orcid.org/0000-0003-4012-1731

[1, 2, 3] Institute of Electrodynamics of the National Academy of Sciences of Ukraine, Kyiv, Ukraine.

An isolated hydroelectric power-generating system of 400 V/50 Hz is studied. The system is built using hydroelectric units equipped with regulated hydraulic turbines and induction generators, a power electronic AC/DC voltage converter, a dump load and a bank of compensating capacitors. The stator windings of the generators in the system under consideration were connected in parallel. The power electronic converter, implemented on fully controlled semiconductor switches, performs the functions of a static synchronous compensator and an active rectifier in the system. A new method for frequency, voltage and load sharing control between generators is proposed. Based on the proposed method, frequency, voltage and load sharing controllers for the discussed system are developed. The converter control is implemented using stator voltage oriented vector control technique and space-vector pulse-width modulation of stator voltage. Verification of the proposed method for frequency, voltage and load sharing control between generators is carried out using the developed dynamic simulation model of the system under consideration. The obtained simulation results were analyzed and further research directions were formulated. Bibl. 23, Fig. 3, Table.

Keywords: *isolated hydroelectric power generating system, hydraulic turbine, active power; load sharing coefficients, parallel operating generators, voltage source converter, regulated dump load, transients.*

РОЗРОБКА ТА ЗАСТОСУВАННЯ МЕТОДУ ЗМІННИХ КОЕФІЦІЄНТІВ ДОЛЬОВОЇ УЧАСТІ ДЛЯ РЕГУЛЮВАННЯ РОЗПОДІЛУ НАВАНТАЖЕННЯ МІЖ АВТОНОМНИМИ ПАРАЛЕЛЬНО ПРАЦЮЮЧИМИ ГЕНЕРАТОРАМИ

Отримано 01 вер. 2025 р.; рекомендовано до публікації 22 вер. 2025 р.
Доступно онлайн 30 вер. 2025 р.

Мазуренко Л. І.[1], Джура О. В.[2], Шихненко М. О.[3]

Автор для кореспонденції: Мазуренко Леонід,
e-mail: 3662491@gmail.com

[1] д-р. тех. наук, проф.
https://orcid.org/00000-0002-7059-249X

[2] канд. техн. наук, ст. наук. співр.
https://orcid.org/0000-0002-0224-3351

[3] канд. техн. наук, наук. співр.
https://orcid.org/0000-0003-4012-1731

[1, 2, 3] Інститут електродинаміки НАН України, м. Київ, Україна.

Розглянуто автономну гідравлічну електрогенерувальну систему 400 В/50 Гц, яка побудована на основі регульованих гідроагрегатів з асинхронними генераторами, напівпровідникового AC/DC перетворювача напруги, регульованого баластного навантаження і батареї компенсаційних конденсаторів. Обмотки статора генераторів у розглянутій системі були з'єднані паралельно. Напівпровідниковий перетворювач, що реалізований на повністю керованих напівпровідникових ключах, у системі виконує функції синхронного статичного компенсатора та активного випрямляча. Запропоновано новий метод регулювання частоти, напруги і розподілу навантаження між генераторами. На основі положень запропонованого методу розроблено алгоритми регулювання частоти, *напруги та розподілу навантаження в системі. Керування перетворювачем реалізовано на основі векторного алгоритму з орієнтацією за результуючим вектором напруги статора та з застосуванням просторово-векторної широтно-імпульсної модуляції статорної напруги. Верифікацію запропонованого методу регулювання частоти, напруги і розподілу навантаження між генераторами проведено з використанням розробленої імітаційної динамічної моделі розглянутої системи. Проведено аналіз отриманих результатів моделювання та визначено подальший напрям досліджень. Бібл. 23, рис. 3, табл. 1.*

Ключові слова: *автономна гідравлічна електрогенерувальна система, гідравлічна турбіна, активна потужність; дольові коефіцієнти, паралельно працюючі генератори, напівпровідниковий перетворювач, регульоване баластне навантаження, перехідні процеси.*

Використані позначення та скорочення

IHPGS – isolated hydroelectric power generation system
BCC – battery of compensating capacitors
AC load – alternating current load
RDL – regulated dump load
GV – guide vane
STATCOM – static synchronous compensator
SVPWM – space vector pulse width modulation
ALSCM – adjustable load sharing coefficients method
SG – synchronous generator
IG – induction generator
VSC – voltage source converter
DC load – direct current load
INDM – imaginary no-droop method
CSM – curve shifting method
DM – droop method
MSM – master-slave method
THD –total harmonic distortion

Introduction. Isolated power generation systems (IPGSs) and microgrids for improving technical and economic performance, using standard equipment, and providing power reserve are typically designed based on more than one source of electrical energy operating in parallel on a direct or alternating current bus [1, 2]. When designing, the possibility of further increasing the IPGS power rating at the modernization stage due to the integration of additional electric power-generating units is also laid down.

Accordingly, experts and scientists, among other things, need to solve the problems of improving the energy efficiency of parallel operating generators and systems [3-7].

IPGSs are built using various energy sources, both renewable and conventional. A stable power supply to local consumers can be provided by IPGSs that have at least one source of stable power generation. Diesel, gas, gasoline, and hydroelectric power units are capable of providing stable and continuous power generation. The construction of isolated hydroelectric power generation systems (IHPGS) requires greater capital investment than diesel power plants and diesel-battery power plants of comparable capacity.However, if sufficient water resources and stable electricity consumption are available, preference should be given to IHPGSs due to their independence from fossil fuels [8].

One way to reduce capital investment in the construction and maintenance of IHPGSs is to use induction generators (IGs), which are less expensive than synchronous generators (SGs) and easier to maintain.

A number of methods have been developed to regulate parallel-operating AC generators. Among them, the droop method (DM), the Curve Shifting Method (CSM), also known as the Droop Compensation Method, and the master-slave method (MSM) should be noted [9-12]. These methods ensure the stabilization of the electrical frequency and voltage in the system, as well as the needed load distribution between the units.

CSM (Droop Compensation Method) was developed to regulate the frequency and voltage of SGs within a power plant operating on a centralized network and to regulate the load sharing between several plants. The advantages of this method are its relative simplicity of implementation and the ability to isochronous (no-droop) frequency and voltage control. CSM can also be used in isolated power systems. According to CSM, the frequency of parallel-operating units is regulated using properly shifted droop characteristics. However, it is also theoretically possible to regulate the frequency of one of the units according to the law f=const, similar to MSM. CSM is considered as a modification of DM. This is explained by the fact that the basis of both DM and CSM is frequency and voltage droop control. But in the case of CSM, droop characteristics are shifted due to additional (secondary) control when the load of the generators changes [13]. Due to this, such shifted droop characteristics are sometimes called imaginary droop characteristics.

The advantage of CSM is the absence of steady state voltage and frequency control errors. Among the disadvantages of CSM, the first one is the no-zero steady state error when at least one of the units is disconnected from the system. Another disadvantage of this method is that its use leads to long-term transients. If these disadvantages are eliminated, the quality of control and, accordingly, the energy conversion efficiency of isolated hydroelectric power generation systems can be improved.

The aim of the work. The aim of the work is to expand the control theory of renewable energy isolated power-generating systems.

Presentation of the main material

1. Schematic solution. The proposed configuration of the IHPGS is shown in Fig. 1. The system shown in Fig. 1 contains hydroelectric power units with regulated hydraulic turbines (HT1, HT2, ... HTn) driving IGs G1, G2, …Gn. The mechanical torque of the HTs is regulated by the control systems of the servo motors of the guide vanes (GVs) GV1, GV2, ... GVn by adjusting the angle references of the GV blades. The stator windings of the generators are connected in parallel. The reactive power required for excitation of the IGs is supplied from two sources, one of which is a battery of compensating capacitors (BCC), and the other is an AC/DC semiconductor voltage source converter (VSC). The VSC acts as a static synchronous compensator (STATCOM) and an active rectifier. A regulated dump load (RDL) is connected to the DC-side of the VSC. The RDL is formed by a series-connected resistor R_{1D} and transistor VT. A DC load shown as a current source is also connected to the DC terminals.

The three-phase AC load of local 400 V/50 Hz electricity consumers is supplied from the stator windings of parallel-operating generators.

The main functions and equations of the VSC, GVs, and the RDL electronic controllers are discussed below.

2. Modification of the curve shifting method

2.1. Development of the adjustable load sharing coefficients method (ALSCM). It should be noted that the above-mentioned CSM was originally called the imaginary no-droop method (INDM), and CSM was just a modification of CSM in [14]. Let's assume that the power generation in an isolated system is equal to the power consumption. Then, under the condition of parallel operation of n electric power units equipped with SGs and operating in an IHPGS, in accordance with CSM, load sharing between generators and no-droop frequency and voltage control are obtained when the control law is used according to the following equations [14, 15]

$$\begin{cases} \Delta f + s_{1P}\left(P1^* - \alpha_{1P}P_{Lsum}\right) = 0 \\ \Delta f + s_{2P}\left(P2^* - \alpha_{2P}P_{Lsum}\right) = 0 \\ \cdot\ \cdot\ \cdot\ \cdot\ \cdot\ \cdot\ \cdot\ \cdot\ \cdot\ \cdot\ \cdot\ \cdot \\ \Delta f + s_{nP}\left(Pn^* - \alpha_{nP}P_{Lsum}\right) = 0 \end{cases}, \tag{1}$$

$$\begin{cases} \Delta U_g + s_{1Q}\left(Q1^* - \alpha_{1Q}Q_{Lsum}\right) = 0 \\ \Delta U_g + s_{2Q}\left(Q2^* - \alpha_{2Q}Q_{Lsum}\right) = 0 \\ \cdot\ \cdot\ \cdot\ \cdot\ \cdot\ \cdot\ \cdot\ \cdot\ \cdot\ \cdot\ \cdot\ \cdot \\ \Delta U_g + s_{nQ}\left(Qn^* - \alpha_{nQ}Q_{Lsum}\right) = 0 \end{cases}, \tag{2}$$

where $s_{jP} < 0$, $s_{jQ} < 0$ - droop coefficients of "active power-frequency" and "reactive power-frequency" droop characteristics of the j-th unit; Pj^*, Qj^* - active and reactive power reference of the j-th unit; $s_{jP} = \dfrac{f_{j2} - f_{j1}}{\Delta Pj}$; $s_{jQ} = \dfrac{U_{gj2} - U_{gj1}}{\Delta Qj}$; f_{j1}, f_{j2}, U_{gj1}, U_{gj2} - the values of frequency and voltage at two arbitrary points 1 and 2 of the above-mentioned static characteristics of the j-th unit; ΔPj; ΔQj - the difference in the values of active and reactive powers between points 1 and 2 of the static characteristics of the j-th unit; $j = \overline{1,n}$; α_{jP}, α_{jQ} - active and reactive power sharing coefficients of the j-th unit; $\sum_{j=1}^{n} \alpha_{jP} = 1$; $\sum_{j=1}^{n} \alpha_{jQ} = 1$; P_{Lsum}, Q_{Lsum} - total active and reactive load of all units of the system; $\Delta f = f^* - f$ - the system output electrical frequency error; f^* - frequency reference; $\Delta U_g = U_g^* - U_g$ - the system output AC voltage error value.

In order to eliminate the above-mentioned shortcomings of CSM, the authors of this article developed an improved method based on CSM for isolated power generation systems built with parallel-operating IGs (Fig. 1). The method was called the adjustable load sharing coefficients method (ALSCM). The essence of the proposed method is that all units of the system participate in the load sharing similar to the CSM, but instead of performing the function of frequency control in the system, they control the power of the regulated dump load. At the same time, the above-mentioned function is assigned to the RDL control system. In addition, in order to eliminate the frequency droop in the system resulting from the failure/disconnection of one or more units, the active load sharing coefficients of the units are properly adjusted.

Provided that *n* electric power units equipped with IGs operate in parallel in an isolated power generation system, in accordance with the ALSCM, proper load distribution between generators and no-droop speed and voltage control are obtained by using the control law described by the following equations

$$Pj_{pu}^* = \frac{\alpha_{jP}}{P_{Nj}}\left(P_{Lsum} + P_{EX}^*\right) - \frac{\beta_j k_I}{\sum_{j=1}^{n} P_{Nj}} \int \left(P_{DL} - P_{EX}^*\right) dt \quad ; \tag{3}$$

$$P_{DL}^* = J_{sum} \frac{k_\omega \dfrac{d\omega_{\max}}{dt} - k_{1\omega}\tilde{\omega}_m - \int k_{2\omega}\tilde{\omega}_m dt}{\omega_{\max}^{-1}} + P_{EX}^* \; ; \tag{4}$$

$$U_g^* = const \, , \tag{5}$$

where k_I, k_ω, $k_{1\omega}$, $k_{2\omega}$ are amplification coefficients; $\omega_{\max} = \max\left(\omega_{m1}, \omega_{m2} \ldots \omega_{mn}\right)$ is the highest rotor speed

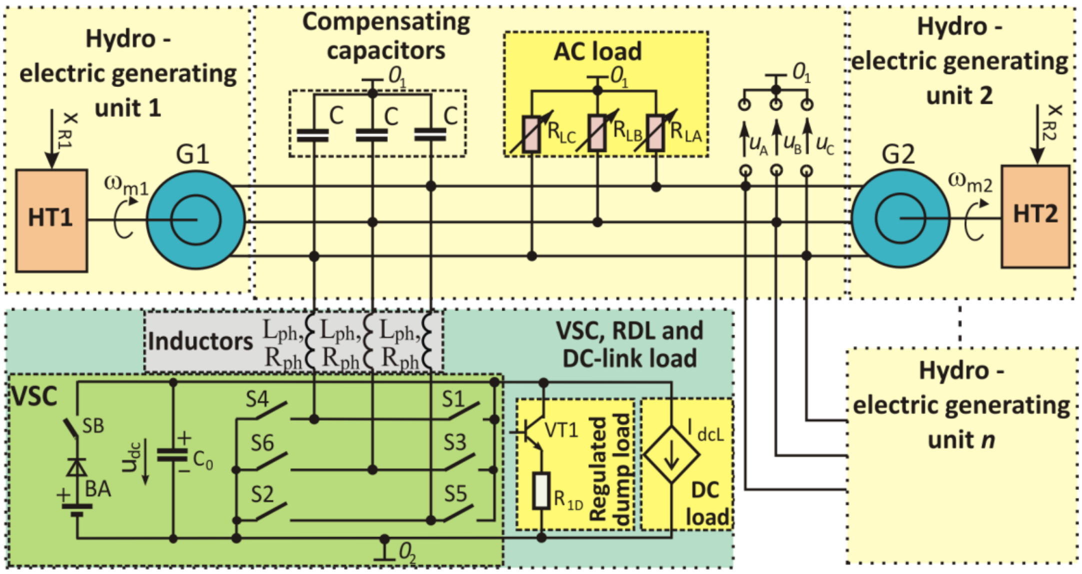

Fig. 1. Schematic diagram of the isolated hydroelectric power generation system

among all generators in the system; $J_{sum} = \sum_{j=1}^{n} J_j$ is the sum of the moments of inertia of all units; P_{EX}^* is the frequency-responsive fast reserve reference of active power in the system; U_g^* is the output AC voltage reference of the system; $\tilde{\omega}_m = \omega_m^* - \omega_{\max}$; ω_m^* - angular speed reference of the generator of the unit with the highest rotor speed; Pj_{pu}^* - IG active power reference of the j-th unit, p.u.; P_{Nj} - IG rated power of the j-th unit; P_{DL}^*, P_{DL} - RDL power reference and actual power values; β_j - RDL quasi-steady state power sharing control coefficient of the j-th unit in the system, $\beta_1 / \alpha_{1P} = \beta_2 / \alpha_{2P} = ... = \beta_n / \alpha_{nP}$; $P_{Lsum} = P_{Lac} + P_{Ldc} / \eta_{VSC}$; P_{Lac}, P_{Ldc} - active power of AC load and DC load of consumers; η_{VSC} - efficiency of the VSC; $j = \overline{1, n}$.

Since IG does not generate reactive power but instead consumes it, there are no equations similar to (2) in the system of equations (3)-(5). The $U_g^* = const$ law is performed by the i_{dI} current controller of the VSC control system. The equation of this controller is given below. The power electronic converter VSC in the system of Fig. 1 performs the functions of a STATCOM [16-18].

In equation (4), instead of the highest rotational speed error, to reduce the number of sensors, the control action can also be the error in the electrical frequency at the system AC output or the error in the angular speed of any unit.

Let us assume that α_{1PB}, α_{2PB}, ... α_{nPB} are the basic active load sharing coefficients of the units in the system, provided that all n units are operating and $\sum_{j=1}^{n} \alpha_{jPB} = 1$. Let's also introduce logical signals "j-th unit is ON/OFF"

$$k_{GUj} = \begin{cases} 1, \text{switching ON of } j-th \text{ unit started} \\ 0, \text{switching OFF of } j-th \text{ unit started} \end{cases}. \quad (6)$$

Then the $\alpha_{1P}, \alpha_{2P}, ... \alpha_{nP}$ values, provided that the ratio of active load sharing coefficients must be equal to the ratio of basic active load sharing coefficients, will be evaluated as follows

$$\alpha_{jP} = \alpha_{jPB} \frac{k_{GUj}}{\sum_{j=1}^{n} \alpha_{jPB} k_{GUj}}, \; j = \overline{1, n}. \quad (7)$$

From (7) it can be seen that if all units are operating, then $\alpha_{jP} = \alpha_{jPB}$, $\forall j \in [1, n]$, and if at least one unit is stopped, then $\alpha_{jP} > \alpha_{jPB}$. Due to the insertion of the adjustable coefficients $\alpha_{1P}, \alpha_{2P}, ... \alpha_{nP}$, the power balance between consumption and generation is maintained, and thus, the no-droop in frequency or speed control is achieved.

The system of equations (3)-(7) is the theoretical basis of the proposed ALSCM method.

If the units are driven by regulated HTs, the GV blades angle reference of the j-th unit can be approximately computed from the following equation

$$c_j^* = \frac{Pj_{pu}^*}{\eta_{Gj} A_{tj}}, \; j = \overline{1, n}, \quad (8)$$

where A_{tj} is the ratio of HT rated power and IG rated power of the j-th unit; η_{Gj} is the IG efficiency of j-th unit.

2.2. Example. For example, let us assume that there are four units in the IHPGS and $\alpha_{1PB} = 0.2$, $\alpha_{2PB} = 0.2$, $\alpha_{3PB} = 0.25$, $\alpha_{4PB} = 0.35$. Let us assume that during the operation of the system, the 1st unit was stopped. Then, after its shutdown, from (7) we obtain $\alpha_{1P} = 0$,

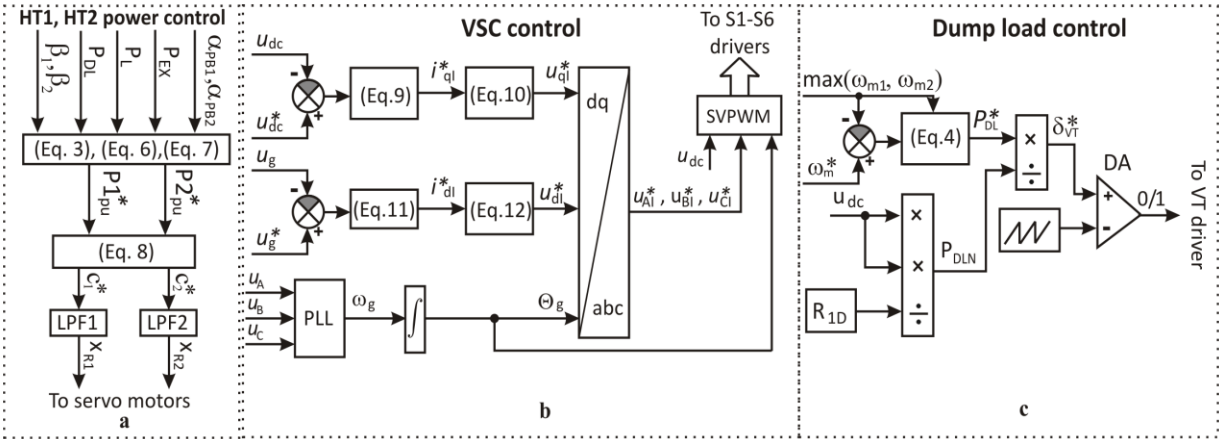

Fig. 2. Block diagram of the HT power control (a), the VSC control (б), the HT speed control (в)

$\alpha_{2P} = 0.2/(0.2+0.25+0.35) = 0.25$,

$\alpha_{3PB} = 0.25/0.8 = 0.3125$, $\alpha_{4PB} = 0.35/0.8 = 0.4375$. Thus, as a result of the shutdown of the first unit, the active power load sharing coefficients of the second, third, and fourth units will be increased by 1.25 times. Due to this, the active power balance between consumption and generation in the system configurations using four and three operating units will be the same.

3. Control of the VSC. The VSC converter control system (Fig. 2b) provides independent DC voltage control of the VSC and the AC stator winding voltage control of the generators. The VSC control algorithm shown in Fig. 2b is similar to that discussed in [19]. The angular position of the IG voltage vector is computed in the PLL (phase-locked loop) block. The equations of the DC voltage controller, AC voltage controller, q-axes, and d-axes VSC current controllers are as follows:

$$i^*_{ql} = -C_0\left(\frac{u_{dc}\delta^*_{VT}}{C_0 R_{1D}} + u^*_{dc} + k_1\tilde{u}_{dc} + \int k_2\tilde{u}_{dc}dt\right)/k_3\,; \quad (9)$$

$$u^*_{ql} = \frac{\dfrac{di^*_{ql}}{dt} + \dfrac{i^*_{ql}R_{ph}}{L_{ph}} + \dfrac{k_{u1} + \int k_{u2}dt}{\left(\tilde{i}_{ql}\right)^{-1}} + \dfrac{v_{gq}}{L_{ph}} + \dfrac{i_{dl}}{\omega_g^{-1}}}{L_{ph}^{-1}}\,; \quad (10)$$

$$i^*_{dl} = k_4\tilde{u}_g + \int k_5\tilde{u}_g dt\,; \quad (11)$$

$$u^*_{dl} = \frac{\dfrac{di^*_{dl}}{dt} + \dfrac{i^*_{dl}R_{ph}}{L_{ph}} + \dfrac{k_{u3} + \int k_{u4}dt}{\left(\tilde{i}_{dl}\right)^{-1}} + \dfrac{v_{gd}}{L_{ph}} - \dfrac{i_{ql}}{\omega_g^{-1}}}{L_{ph}^{-1}}\,, \quad (12)$$

where δ^*_{VT} – duty cycle reference of the VT control signal; $\tilde{u}_{dc} = u^*_{dc} - u_{dc}$; $\tilde{i}_{ql} = i^*_{ql} - i_{ql}$; $\tilde{i}_{dl} = i^*_{dl} - i_{dl}$; i_{ql}, i_{dl}, v_{gq}, v_{gd} are q-axes and d-axes components of the VSC current and AC load voltage; ω_g – angular frequency of the AC load voltage; k_1, k_2, k_3, k_4, k_5, k_{u1}, k_{u2}, k_{u3}, k_{u4} are constants. The logic signals for the VSC transistors control are formed by a space vector pulse width modulation (SVPWM) unit.

4. RDL control. The block diagram of the RDL control algorithm for n=2 units is shown in Fig. 2c. As a control action of the RDL controller, it was decided to use the angular speed error of the generator of the unit with the highest rotor speed in the system. The duty cycle reference δ^*_{VT} of the VT control signal is computed as the ratio of the dump load power reference (continuously computed) to its rated power. The RDL power reference is obtained using equation (4).

5. HT control. The block diagram of the HT power control algorithm for n=2 units is shown in Fig. 2a. Low-pass filters LPF1, LPF2 are used to attenuate the high-frequency component of the output signal. As can be seen from Fig. 2a, the GV blades angle control in HT1 and HT2 hydro turbines is implemented using equations (3), (6), (7) and (8).

6. Digital simulation settings. Complex mathematical models of electromechanical systems are often implemented in simulation environments, such as MATLAB. This computing platform is considered a powerful and effective tool for theoretical investigations [20].

The proposed IHPGS (Fig. 1) was numerically investigated using the MATLAB/Simulink software environment in configuration with n=2 units.

Generators G1 and G2 were represented by a fourth-order dynamic model during the numerical studies [21].

HT1 and HT2 were modeled without a surge tank by a differential-algebraic system of equations [22].

$$P_{HTj,pu} = A_{tj}h_j(q_j - q_{jnl}) - D_jc_j\Delta\omega_{mj}\,; \quad (13)$$

$$\frac{dq_j}{dt} = \frac{1 - h_{lj} - h_j}{T_{Wj}}, \quad (14)$$

$$W_{Sj}(p) = c_j / x_{Rj} = 1/\left(1 + p/k_{Aj} + p^2 T_{Aj}/k_{Aj}\right), \quad (15)$$

where $P_{HTj,pu}$ is HTj power, p.u.; h_j is pressure head, p.u.; q_j and q_{jnl} are flow rate and no load flow, p.u.; h_{lj} – head loss due to friction in theconduit, p.u.; $\Delta\omega_{mj} = \omega_{mj} - 1$ is the HT speed deviation from 1 p.u.; T_{Wj} is time constant of the conduit, s; $q_j = c_j \sqrt{h_j}$; c_j is the GV blades angle; D_j is the HT damping coefficient; $W_{Sj}(p)$ is the GV servo motor transfer function; $p = d/dt$; x_{Rj} – input signal of the servo motor formed by the HT speed controller; k_{Aj}, T_{Aj} – gain coefficient and time constant of the servo motor and GV blades; $j = \overline{1,2}$.

The characteristics and parameters of the electromechanical systems of unit 1 and unit 2 were assumed to be identical.

Hydro turbines HT1, HT2

Nominal power: 30 kW; time constant of the conduit $T_{W1} = T_{W2}$ =1 c; $A_{t1} = A_{t2}$ =1.073; $D_1 = D_2$ =0; $k_{A1} = k_{A2}$ = 3.33; $T_{A1} = T_{A2}$ =0.07 s; no load flow $q_{1nl} = q_{2nl}$ =0 p.u.; head loss due to friction in the conduit $h_{l1} = h_{l2}$ =0 p.u.; GV blades speed limits: ±0.2 p.u./s.

Generators G1 and G2

Rated power/voltage (connection): 30 kVA/400 V (Y); rated speed/number of pole pairs: 1500 rpm/2; active resistance of stator/rotor phase: 0.143 Ω/0.08 Ω; stator and rotor leakage inductance: 0.00115 H; IG and HT rotating mass inertia constant: 2 s; friction factor: 0.027 N·m·s/rad. The magnetization characteristic of IGs is shown in the table below.

Table. Magnetization characteristic of IGs

Phase current, A	3	6	11	15	20	30	44	62	120
Line voltage, V	192	270	345	384	422	460	498	536	600

Load, inductors and capacitors

The DC side dump load resistance $R_{1D} = 19$ Ω; VT resistance in ON/OFF state = 0.001 Ohm / 100 kOhm; AC load is resistive symmetrical; DC load power = 0.02 kW; active resistance of inductors $R_{ph} = 0.041$ Ω; inductance of inductors $L_{ph} = 0.00068$ H; $C_0 = 0.04$ F; rated power/rated voltage/connection of compensating capacitors: 8 kVA/400V/Y_n.

Base quantities of power, voltage, current, frequency and speed for Fig. 3 transients

30 kVA = 1 p.u. of power; 230 V = 1 p.u. of root mean square voltage; $61.2/\sqrt{2}$ A = 1 p.u. of IG rms phase current; 770 V = 1 p.u. of DC side voltage; 50 Hz = 1 p.u. of electrical frequency; 1500 rpm = 1 p.u. of speed.

SVPWM vector control system of the VSC

Carrier frequency = 9 kHz; k_1=60; k_2=900; k_3=1.5; k_4=10 , k_5=25; k_{u1}=1540; k_{u2}=640000; k_{u3}=1540; k_{u4}=640000; RMS phase voltage reference of IGs = 1.04 p.u.; DC side voltage reference of the VSC = 1 p.u.

Controllers of GVs of hydraulic turbines

k_I=2; $\alpha_{1P} = \alpha_{1PB}$=0.767; $\alpha_{2P} = \alpha_{2PB}$=0.233; β_1=0.256; β_2=0.0778; $\eta_{G1} = \eta_{G2}$=0.9; the values of the $\left(\beta_j k_I / \sum_{j=1}^{n} P_{Nj}\right) \cdot \int \left(P_{DL} - P_{EX}^*\right) dt$ component in equation (3) were limited by the range $[-0.125,\ 0.125]$.

RDL control system

Switching frequency = 2 kHz; differential, proportional, and integral gain of the frequency controller: k_ω=0.68, $k_{1\omega}$ = 272, $k_{2\omega}$ = 5.1; the frequency-responsive fast reserve of active power reference in the system P_{EX}^* = 8.7 kW; ω_m^* =1.02 p.u.

7. Analysis of simulation results. Simulation results of the Fig. 1 system are shown in Fig. 3.

As can be seen from Fig. 3a, until the moment of time $t = 4.4\ c$ the IHPGS operated in a quasi-steady state. The total active load of consumers was 0.108 p.u. = 3.24 kW and the RDL power was 0.29 p.u. = 8.7 kW. The values of active power generated by IGs G1 and G2 were equal 0.344 p.u. and 0.09 p.u. (Fig. 3b), respectively. Thus, the ratio of the active powers of the IGs was 3.82, while the ratio of the active power sharing reference coefficients of the units was slightly lower, namely: $\alpha_{1P} : \alpha_{2P}$ =0.767:0.233=3.29. The difference in ratio values is due to the low load power and the influence of losses in the IGs (the actual efficiencies of G1 and G2 differed due to their different loadings) on the precision of load sharing. The VSC active power corresponded to the active power of the RDL.

The speeds of IGs G1 and G2 were 1.02 p.u. and 1.0155 p.u., respectively, and the electrical frequency in the system was 1.0137 p.u. (Fig. 3d).

The reactive power consumption of IG G1 and IG G2 did not differ significantly and amounted to 0.467 p.u. and 0.435 p.u., respectively (Fig. 3c). Most of the reactive power that had been consumed by both IGs came from the VSC (0.604 p.u. = 18.12 kVA), and the rest was provided by the BCC.

The GV blades' angle reference (Fig. 3e) in unit 1 was 0.351 p.u., in unit 2 – 0.107 p.u., and their ratio was 3.28, being close to the ratio reference $\alpha_{1P} : \alpha_{2P}$.

The RMS phase current value of the IG G1 stator winding was 0.543 p.u., that is 0.122 p.u. higher than in G2 due to the different loadings of the generators.

The RMS value of the IGs phase voltage and the rectified voltage magnitude of the VSC were equal to the reference values of 1.04 p.u. = 239.2 V and 1 p.u. = 770 V, respectively (Fig. 3f).

The THD coefficient of the IGs phase voltage was around 2% (Fig. 3h).

At the moment of time $t = 4.4\ c$, the admittance of the AC load increased. Due to this, AC load active power reached a value of 0.324 p.u. = 9.73 kW.

As a result of the rapid increase in the AC load, the mechanical rotational speed in both units and the electrical frequency of the system began to decrease (Fig. 3d), as well as the power of the RDL (Fig. 3a).

The GV blades' angle reference (Fig. 3e) in unit 1 was increased by the GV controller of HT1 to 0.537 p.u. with a subsequent slow decrease to 0.517 p.u. In unit 2, the GV blades' angle reference was increased to 0.164 p.u. and then slightly reduced to 0.157 p.u. as a result of adjusting the $\left(\beta_j k_I / \sum_{j=1}^{n} P_{Nj}\right) \cdot \int \left(P_{DL} - P_{EX}^{*}\right) dt$ component in equation (3) of the HT power controller (Fig. 2a).

At the end of the transient process caused by the increase in consumer load, the ratio of active powers of IG G1 and IG G2 settled at 0.520 p.u./ 0.1435 p.u. = 3.62. Comparing this value with the corresponding value of 3.82 at the interval before load increase, it can be seen that the active load sharing between IGs became more approximate to the ratio reference value of 3.29.

As can be seen from Fig. 3d, the speed and frequency transients in the system faded away in 1.5–1.6 s, that is nearly 10 times quicker than that of an isolated hydroelectric unit equipped with a SG and speed control using solely the GV controller [23].

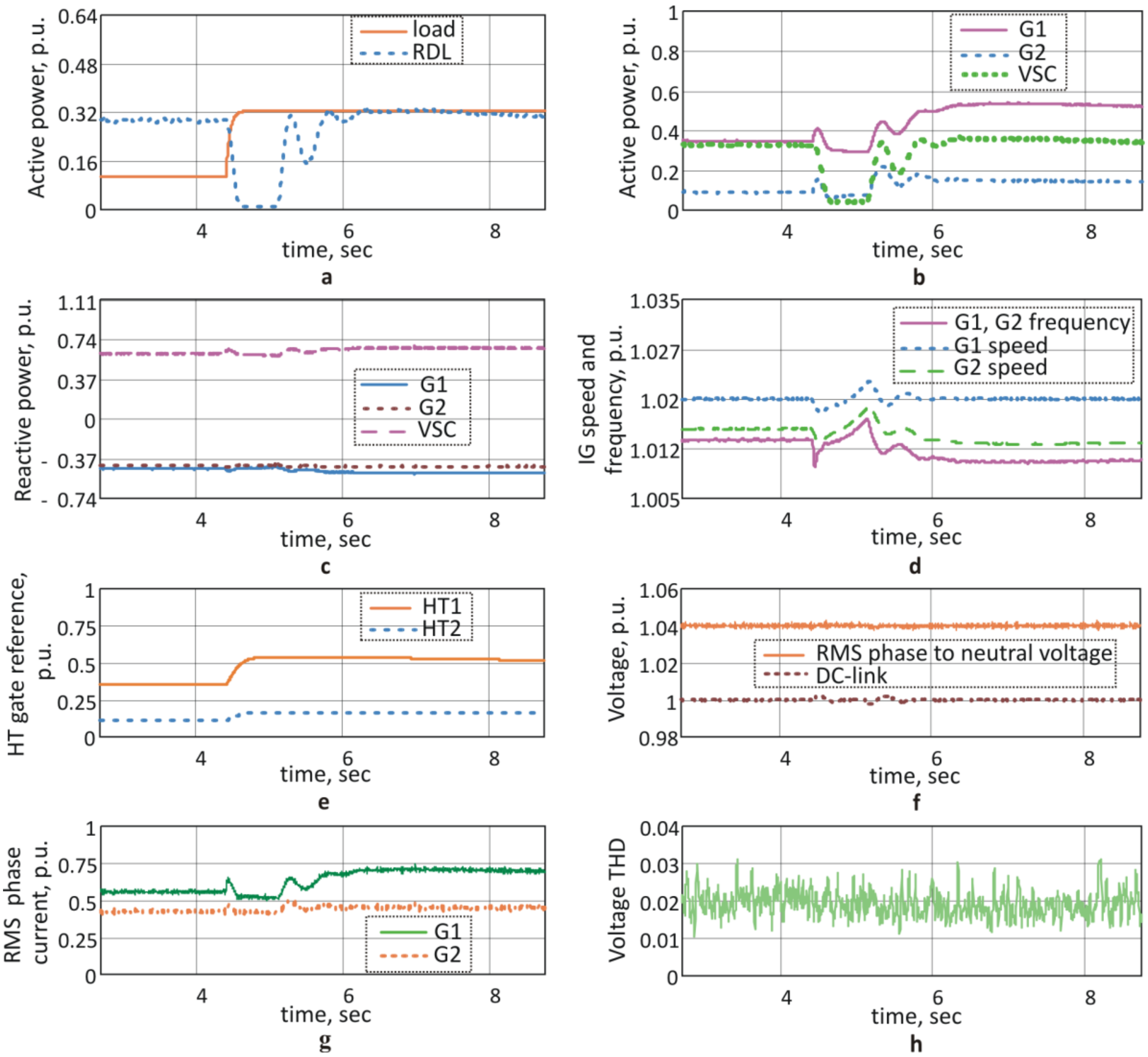

Fig. 3. Electromechanical transients in the system of Fig. 1 for two isolated hydroelectric power units operating in parallel

The maximum RMS phase voltage error of IGs during the transient process in the system was 0.29% of the rated voltage value, and the VSC maximum rectified voltage error was 0.23% of the DC voltage reference.

The power of the RDL at the end of the simulation interval was nearly equal to the RDL power magnitude that was before the increase in consumer load (Fig. 3a).

As a result of performing by GVs and RDL controllers their control actions, the IG G1 speed settled at the value that was before AC load increase, that is 1.02 p.u. At the same time, the IG G2 speed and the electrical frequency in the system decreased slightly to 1.0134 p.u. and 1.0106 p.u. respectively in accordance with equation (4).

The value of the IGs output voltage THD did not change significantly with an increase in load (Fig. 3h).

Conclusions. A new adjustable load-sharing coefficients method for frequency and voltage control in IHPGSs using parallel operating induction generators has been developed. Due to this, further advancement in control theory of renewable energy isolated power-generating systems was attained. The results of numerical simulation of the proposed isolatedpower generation system built with two parallel-operating hydroelectric power units equipped with IGs of 30 kVA rated power, allowed for preliminary verification of the proposed adjustable load sharing coefficients method. The implementation of the control strategy for HT guide vanes, regulated dump load, and voltage source converter based on the statements of the proposed method allowed to achieve no-droop control of voltage, the rotational speed of one of the units, and quasi-steady state power of the regulated dump load in the system.

Based on the analysis of the electromechanical transients of the system obtained during a stepwise increase in the load of consumers by 11% of the total rated power of the generators, it was specified that the decay time of speed and frequency transients did not exceed 1.5–1.6 s. This is a good result due to a 10 times shorter transient time compared to an isolated hydroelectric unit investigated by other scientists, equipped with an SG and speed control implemented solely with the GV controller.

It was also found that the implementation of the proposed adjustable load sharing coefficients method led to active load sharing between generators with an error. The magnitude of this error for a consumer load of 3.24 kW (5.4% of the total rated power of the generators) was 16%, and for a consumer load of 9.73 kW (16.2% of the total rated power of the generators), it was 10%. This error is explained by the fact that the proposed method provides control of the ratio of the mechanical powers of the generators in accordance with the load-sharing reference coefficients. As a result, losses in the IGs in load sharing control are not taken into account, thus affecting the accuracy of the active load sharing between the units.

Further investigations are planned to focus on more thorough studies of the considered isolated hydroelectric power generation system with two or more units and on improving the accuracy of load sharing between units.

This work was supported by the NATIONAL RESEARCH FOUNDATION OF UKRAINE [PROJECT "Electromechanical systems of increased energy efficiency for energy, technologies and transport", № 2023.04/0075].

REFERENCES

1. Yang J., Wang Q., Miao X., Yu Y., Wei M. and Ye L., "Review on Equivalent Modeling for Islanded Systems with Distributed Power Generation Integration," 2024 9th Asia Conference on Power and Electrical Engineering (ACPEE), Shanghai, China, 2024, pp. 1248-1253, doi: https://doi.org/10.1109/ACPEE60788.2024.10532408.
2. Kozak M., "Alternating Current Electric Generator Machine Inverters in a Parallel Power Sharing Connection," in IEEE Access, vol. 7, pp. 32154-32165, 2019, doi: https://doi.org/10.1109/ACCESS.2019.2902647.
3. Choi, E.; Kim, H. Advanced Energy Management System for Generator–Battery Hybrid Power System in Ships: A Novel Approach with Optimal Control Algorithms. J. Mar. Sci. Eng. 2024, 12, 1755. https://doi.org/10.3390/jmse12101755.
4. Peng Y., Zhang X. and Zhan L., "Transient Load Sharing between Grid-forming Generators in Islanded Microgrid," 2020 IEEE Energy Conversion Congress and Exposition (ECCE), Detroit, MI, USA, 2020, pp. 3867-3871, doi: https://doi.org/10.1109/ECCE44975.2020.9236390.
5. Artemenko M. Y., Kutafin Y. V., Shapoval I. A., Chopyk V. V., Mykhalskyi V. M. and Polishchuk S. Y., "Integral Strategies of Active Filtration in the Reference Frame of the Two-Wattmeters Method," IEEE EUROCON 2021 - 19th International Conference on Smart Technologies, Lviv, Ukraine, 2021, pp. 508-512, doi: https://doi.org/10.1109/EUROCON52738.2021.9535637.
6. Logeshwari V., Chitra N., Kumar A. S., Munda J., Optimal Power Sharing for Microgrid with Multiple Distributed Generators, Procedia Engineering, Volume 64, 2013, pp. 546-551, ISSN 1877-7058, https://doi.org/10.1016/j.proeng.2013.09.129.
7. Zargar MY, Mufti MD, Lone SA. Dynamic performance improvement of isolated power system using intelligently controlled SMES. IET Gener Transm Distrib. 2021; 15: 408-419. https://doi.org/10.1049/gtd2.12029.
8. Mazurenko L. I., Dzhura O. V., Shykhnenko M. O., Kotsiuruba A. V. “Modification of the master generator method used for frequency and voltage control in isolated power systems with parallel operating AC generators,” Tekhnichna Electrodynamica, No. 2. pp. 28–36, 2023, doi: https://doi.org/10.15407/techned2023.02.028.

9. Ndeh S. G., Ebot B. J., Akawung A. F., Khan N. D. and Emmanuel T., "Decentralized Droop Control Strategies for Parallel-Connected Distributed Generators in an AC Islanded Microgrid: A Review," 2023 7th International Conference on Green Energy and Applications (ICGEA), Singapore, Singapore, 2023, pp. 83-90, doi: https://doi.org/10.1109/ICGEA57077.2023.10126012.

10. Rocabert J., Luna A., Blaabjerg F. and Rodríguez P., "Control of Power Converters in AC Microgrids," in IEEE Transactions on Power Electronics, vol. 27, No. 11, pp. 4734-4749, Nov. 2012, doi: https://doi.org/10.1109/TPEL.2012.2199334.

11. Li C., Chaudhary S. K., Savaghebi M., Vasquez J. C. and Guerrero J. M., "Power Flow Analysis for Low-Voltage AC and DC Microgrids Considering Droop Control and Virtual Impedance," in IEEE Transactions on Smart Grid, vol. 8, no. 6, pp. 2754-2764, Nov. 2017, doi: https://doi.org/10.1109/TSG.2016.2537402.

12. Jeong, B.-c. Modified Master–Slave Controller for Stable Power Supply of Energy Storage Based Microgrid. Energies 2022, 15, 4245. https://doi.org/10.3390/en15124245.

13. Vadi, S.; Padmanaban, S.; Bayindir, R.; Blaabjerg, F.; Mihet-Popa, L. A Review on Optimization and Control Methods Used to Provide Transient Stability in Microgrids. Energies 2019, 12, 3582. https://doi.org/10.3390/en12183582.

14. Moskalev A.G. Automatic regulation of the power system mode by frequency and active power. M.-L. Gosenergoizdat. 1960. 241 s. [RU].

15. Iandulskyi O. S., Steliuk A. O., Lukash M. P. Automatic control of frequency and active power flows in power systems [Text]: training manual. K. NTUU «KPI», 2009. 98 s. [in Ukr].

16. Chermiti D. and Khedher A., "Voltage and Frequency Control of a Self-Excited Induction Generator using Bidirectional STATCOM Devoted to Rural Electrification," 2019 10th International Renewable Energy Congress (IREC), Sousse, Tunisia, 2019, pp. 1-6, doi: https://doi.org/10.1109/IREC.2019.8754570.

17. Iannuzzi D., Lauria D. and Pagano M., "Advanced Statcom Control for Stand Alone Induction Generator Power Sources," 2008 International Symposium on Power Electronics, Electrical Drives, Automation and Motion, Ischia, Italy, 2008, pp. 60-65, doi: https://doi.org/10.1109/SPEEDHAM.2008.4581064.

18. Satpathy, A.S., Kastha, D. and Kishore, K. (2019), Control of a STATCOM-assisted self-excited induction generator-based WECS feeding non-linear three-phase and single-phase loads. IET Power Electronics, 12: 829-839. https://doi.org/10.1049/iet-pel.2018.5482.

19. L. I. Mazurenko, O. V. Dzhura, A. V. Kotsiuruba and M. O. Shykhnenko, "A Wind-Hydro Power System Using a Back-to-Back PWM Converter and Parallel Operated Induction Generators," 2020 IEEE Problems of Automated Electrodrive. Theory and Practice (PAEP), 2020, pp. 1-5, doi: https://doi.org/10.1109/PAEP49887.2020.9240777.

20. Popovych O. M., Holovan I. V. A simulation model of a hydro turbine for complex modeling of the electromechanical system of a hydroelectric power station. Vidnovliuvana enerhetyka. 2023. No 2. S.51–60. https://doi.org/10.36296/1819-8058.2023.2(73).51-60. [in Ukr].

21. Krause P. C.; Wasynczuk O.; Sudhoff S. D., Analysis of Electric Machinery and Drive Systems, Wiley-IEEE Press, 2002, P. 632. doi: https://doi.org/10.1109/9780470544167.

22. Mazurenko L. I., Kotsiuruba A. V., Dzhura O. V. and Shykhnenko M. O., "Voltage and Power Regulation of an Induction Generator-Based Hydroelectric Power Plant," 2021 IEEE International Conference on Modern Electrical and Energy Systems (MEES), 2021, pp. 1-6, doi: https://doi.org/10.1109/MEES52427.2021.9598549.

23. Sebastián R. and Quesada J., "Modeling and simulation of an isolated wind Hydro Power System,"IECON 2016 - 42nd Annual Conference of the IEEE Industrial Electronics Society, Florence, 2016, pp. 4169-4174, doi: https://doi.org/10.1109/IECON.2016.7793992.